J. Biochem. 119, 731-736 (1996)

Pore Formation on Proliferating Yeast *Saccharomyces cerevisiae* Cell Buds by HM-1 Killer Toxin

Tadazumi Komiyama,*[,1] Tatsuo Ohta,* Hiroshi Urakami,* Yasuhiko Shiratori,† Tsuyoshi Takasuka,† Misako Satoh,‡ Takahide Watanabe,† and Yasuhiro Furuichi‡

*Department of Biochemistry, Niigata College of Pharmacy, 5-13-2 Kamishinei-cho, Niigata 950-21; †Department of Molecular Genetics, Nippon Roche Research Center, Kajiwara, Kamakura 247; and ‡AGENE Research Institute, Kajiwara, Kamakura 247

Received for publication, October 23, 1995

The cytocidal effect of HM-1 produced by *Hansenula mrakii* on yeast *Saccharomyces cerevisiae* cells was studied. The HM-1 strongly inhibited the growth of *S. cerevisiae* cells at a low concentration (IC_{50}: 2.1×10^{-8} M) by reducing the number of viable cells. The killer action of HM-1 was most efficient when cells were actively proliferating. Cells in a resting state were resistant, but they became HM-1-sensitive after about 90 min of culturing at 30°C, concomitantly with the increment of budding index. In association with the reduction of viable cell number, ultraviolet light-absorbing cellular components were discharged from sensitive cells. HM-1 molecules appear to bind to susceptible cells rather loosely since cells incubated with HM-1 were able to proliferate after having been washed. By phase-contrast light microscopy and scanning electron microscopy, discharge of cell material was observed at the budding portions of HM-1-treated cells. Addition of sorbitol to make the culture medium isotonic partially reduced the cell death induced by HM-1. These results suggest that HM-1 acts on the budding region of proliferating yeast cells, resulting in pore formation, leakage of cell material and eventual cell death.

Key words: antifungal drug, killer toxin, β-glucan synthase, budding, cell wall, yeast proliferation.

Since the discovery that yeast has a cytocidal ability (*1*), a number of cytocidal proteins originating from microorganisms have been identified and designated as killer toxins. Molecular mechanisms underlying the killing action have been elucidated for several killer toxins. The K1 killer toxin produced from certain strains of *Saccharomyces cerevisiae* is coded for by a double-stranded RNA plasmid gene and inhibits the pumping of protons in the sensitive cells (*2, 3*). A killer toxin produced by *Kluyveromyces lacits* harboring a linear double-stranded DNA plasmid and inhibiting the adenylate cyclase activity of sensitive yeast (*4, 5*) has been shown in a recent study to have an essential protein kinase activity (*6*). Another killer toxin from *Pchia kluyveri* has been shown to form pores in the lipid bilayer (*7*).

The HM-1 killer toxin (referred to hereafter as HM-1) excreted by the yeast *Hansenula mrakii* is an example of such killer toxins of low molecular weight, around 10,000 Da (*8*). The gene of HM-1 exists in chromosomal DNA. Biochemical and microbiological studies have demonstrated that HM-1 has the following unique features: it consists of 88 amino acid residues rich in cysteine (10 cysteines per molecule), it is a hydrophobic protein stable to heat (100°C, 10 min) and a wide range of pH values (pH 2.0-11.0), and it exerts a strong cytocidal effect on sensitive yeast and fungal cells. Its cytocidal effect has been suggested to involve the inhibition of β-(1,3)-glucan synthase (*8, 9*), but this hypothesis has not yet been substantiated.

In this report, we describe the mode of action by which HM-1 kills *S. cerevisiae* cells. Some of its properties are compared with those of aculeacin A and papulacandin B, lipophilic antibiotics known to inhibit cell wall β-(1,3)-glucan synthesis (*10, 11*). The results obtained from these studies indicate that the cytocidal effect of HM-1 is cell growth-dependent, and involves a release of cellular components through pores formed on growing buds.

MATERIALS AND METHODS

Materials—HM-1 was purified from the culture media of *H. mrakii* (IFO 0895) as reported previously (*12, 13*). *S. cerevisiae* A451 was used as the test cell line and 1.0 absorbance unit at 600 nm was calculated to be equivalent to 2×10^7 cells/ml.

Bacto yeast extract, bacto-peptone, and yeast nitrogen base were obtained from Difco Laboratories (Detroit, MI, USA). Aculeacin A (*14*) and papulacandin B (*15*) were donated by Asahi Kasei (Ooni, Shizuoka) and Ciba-Geigy (Basle, Switzerland), respectively. A light microscope (model BHS) and an electron microscope (JEM-100CX) manufactured by Olympus Optical (Tokyo) and JEOL

[1] To whom correspondence should be addressed. Tel: +81-25-269-1224, Fax: +81-25-268-1230, E-Mail: komiyam@niigata-pharm.ac.jp

Abbreviations: HM-1, a killer toxin produced by *Hansenula mrakii*; PBS(+) and PBS(−), Dulbecco's phosphate-buffered saline with and without $CaCl_2$ and $MgCl_2$, respectively; IC_{50}, inhibitory concentration that yields 50% inhibition of cell growth.

(Tokyo), respectively, were used.

Methods—*S. cerevisiae* cells were incubated and grown in YPD medium consisting of 1% yeast extract and 2% each of peptone and glucose. Cells growing in the logarithmic phase were usually used for the experiments.

The killer activity was measured by monitoring the viability of HM-1-treated cells. The plate assay method was used, in which *S. cerevisiae* cells and various amounts of HM-1 were incubated at 30°C for 40 min in YPD medium, followed by 100-fold dilution with the same medium and layering on YPD agar plates. After culturing for two nights at 30°C, the number of colonies was counted. In the liquid culture method, which is much quicker than the plate assay, *S. cerevisiae* cells (4×10^6 cells/ml) were cultured with various amounts of HM-1 in YPD medium at 30°C with shaking at 175 rpm for 14 h. The viability of the cells was then monitored by measuring the absorbance at 600 nm.

Another method was used to monitor the killer activity based on the liquid culture method (measurement of viable cells in liquid culture medium): *S. cerevisiae* (1.3×10^7 cells/ml) cells were incubated with 4 μg/ml HM-1 in YPD medium at 30°C for the indicated time. After incubation, 5 μl of the mixture was transferred to 2.0 ml of YPD medium and cultured with shaking at 175 rpm at 30°C. The number of cells grown after 18-21 h of culturing was then measured in terms of the absorbance of 600 nm.

Budding Index—Budding index of cells was determined microscopically in the absence of HM-1, and expressed as the percentage of the cells budding with respect to total cells. In the case of rapidly growing cells, the cells were segregated by sonication at 100 W for 10 s before the determination.

Measurement of the Leakage of Ultraviolet Light-Absorbing Material into the Medium—*S. cerevisiae* cells (5×10^7 cells/ml) in logarithmic growth phase or in the resting state were incubated with 4 μg/ml of HM-1 in medium containing 0.7% yeast nitrogen base and 2% glucose. At the indicated sampling times, 250 μl of the mixture was removed and centrifuged at 12,000 rpm for 15 s. The supernatants were passed through a cellulose acetate filter (pore size 0.45 μm) to remove turbidity, and the difference spectrum between the samples of 0 time and each sampling time was measured.

Light Microscopy—*S. cerevisiae* cells (4×10^7 cells/ml) were incubated with 4 μg/ml HM-1 in YPD medium with shaking at 175 rpm at 30°C for 3 h. The cells were stained with 0.1% methylene blue containing 0.8 M sorbitol and were photographed under a phase-contrast microscope using immersion oil.

Scanning Electron Microscopy—*S. cerevisiae* cells (2×10^7 cells/ml) were incubated at 37°C with or without 4 μg/ml HM-1 in YPD medium with shaking at 175 rpm for 3 h. The cells were collected by centrifugation and were resuspended in PBS(−). This cell washing step was repeated three times and the washed cells were finally suspended in PBS(−). Fixation was carried out as follows: cells were treated successively with 2% glutaraldehyde in PBS(+) at 4°C for 2 h, with 2% osmium tetroxide at 4°C for 2 h and with 0.25% ruthenium tetroxide at 25°C for 5 min. They were then dehydrated in ethanol, transferred to isoamyl acetate and dried by the critical point drying method. The specimens were coated with gold using an ion sputter and were examined under an electron microscope in the scanning mode at 20 kV.

RESULTS

Cytocidal Effect of HM-1 Toxin—The viability of the cells was measured by plate assay using *S. cerevisiae* (strain A451). Figure 1 shows that the number of cell colonies viable on agar plate decreased by more than 80% after 40 min incubation with 0.5 μg/ml HM-1 (Panel B), and at higher concentrations of HM-1 most of the cells were unable to grow (Panels C and D). Prolonged culturing (over 5 days) failed to regain viable cells on the same agar plates, on which HM-1-untreated cells were able to grow well (Panel A). These results clearly indicate that low concentrations of about 5×10^{-8} M HM-1 kill a majority of *S. cerevisiae* cells after contact for 40 min. Similar experiments to study the cause of this cytocidal effect were carried out by culturing the HM-1-treated cells in liquid YPD medium. Yeast cells incubated with varying concentrations of HM-1 were freed from HM-1 by 100-fold dilution, and cultured overnight under the optimal conditions of cell growth. The degree of the cytocidal effect was then assessed conveniently by measuring the turbidity of the cultured cells.

Conditions That Affect the Cytocide—Effects of temperature, treatment time and/or the state of the cells (growing or resting) were studied in relation to the degree of cytocidical activity of HM-1. First, the effect of temperature was analyzed. In the experiments, cells in the logarithmic growth phase were used. They were incubated at various temperatures (0, 20, 30, and 37°C), and after 20, 40, 60, 90, 120, and 150 min of incubation, a portion of the

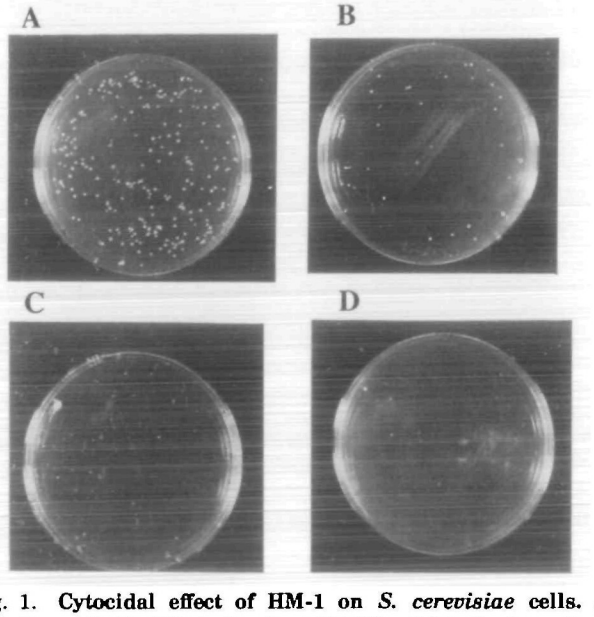

Fig. 1. **Cytocidal effect of HM-1 on *S. cerevisiae* cells.** *S. cerevisiae* cells (A 451 strain, about 3×10^6 cells) in the logarithmic growth phase were incubated (30°C for 40 min) in YPD medium with purified HM-1 at the indicated concentrations. After incubation, the cells were diluted 100-fold with fresh YPD medium and portions of the cells were placed on agar plates prepared with YPD medium. Culturing was performed at 30°C for 36 h. A, 0 μg/ml HM-1, B, 0.5 μg/ml HM-1; C, 1 μg/ml HM-1; D, 3 μg/ml HM-1.

cells was removed and cultured in the absence of HM-1 overnight. Figure 2A clearly shows that the optimum incubation temperature for the cytocidal effect by HM-1 was 30°C, followed in order by 20 and 37°C. Nearly 90% of the cells were killed after 40 min incubation at this optimal temperature: a condition which provided cells with a budding index as high as 80-90% (Fig. 2, A and B, closed symbols). When the cells were stained with methylene blue, the number of blue-stained cells increased with time, and some of these cells were spouting at the budding position as described later in more detail. In contrast, incubation at 0°C produced only a limited cytocidal effect. These results demonstrated that HM-1 exerts its greatest activity when incubated with cells at the temperature optimal for cell growth.

Figure 2B shows the results of similar experiments using cells in the resting state. As with growing cells, cells in the resting state were also killed by HM-1 toxin. However, a longer incubation was required before the onset of cell death. Prior incubations of 90 and 180 min at 30 and 37°C, and 20°C, respectively, were needed for the cells to become sensitive to HM-1. A simultaneous increment of budding index was also observed under these incubation conditions. Cells incubated with HM-1 at 0°C and cultured at 30°C after dilution did not die. Since the cell cycle time of yeast cells (strain A451) is 90 min at 30°C in the YPD medium, our results show that HM-1 exerts its toxic activity only on growing cells. The minimum concentration and the 50%-inhibitory concentration (IC_{50}) (*i.e.*, 50% of the cell population killed) were determined under the optimal conditions identified by us in the experiments above (Fig. 3). The IC_{50} was calculated as 2.1×10^{-8} M (0.2 μg/ml). Concentrations lower than 0.07 μg/ml did not affect the overall cell growth.

Leakage of Cellular Components from HM-1-Affected Cells—As leakage of cellular components was predicted based on the microscopic observation of HM-1-treated cells, the changes in UV absorption of the medium were measured during incubation with HM-1. As shown in Fig. 4A, the UV_{258nm}-absorbing material was discharged from the logarithmically growing cells as the cytocidal effect of HM-1 was manifested. The UV_{258nm}-absorbing material did not appear in the medium containing resting cells until about 90 min from the start of incubation, while it appeared thereafter as the cytocidal effect of HM-1 was manifested. This material showed a maximum UV absorption at 257-258 nm as determined from the difference spectrum, and contained tRNAs, as discussed later. These results suggest that HM-1 seems to generate pores in *S. cerevisiae* cells.

Features of HM-1 Binding to Sensitive Cells—Since HM-1 is cytocidal to sensitive yeast cells at very low concentrations, we investigated its binding ability to the cells. Using a liquid culture assay, the effect of washing was examined. As with the experiments shown in Fig. 2, growing yeast cells were incubated with a lethal dose of HM-1 (4 μg/ml), and portions of the cells were removed after incubating for 0, 30, and 40 min, centrifuged, resuspended in YPD medium, and cultured overnight to measure the viability of the cells. For comparison, similar experiments were performed with the antibiotics aculeacin A (24 μg/ml) and papulacandin B (20 μg/ml), which are strong antifungal agents (*14, 15*). Figure 5A shows that (i) most cells without washing (designated as *control* in the legend) died as described before (Fig. 2A); (ii) cells washed immediately after contact with HM-1 were as viable as untreated cells; and (iii) cells which were washed after 30 or 40 min of contact with HM-1 showed reduced viability. These results suggest that HM-1 binds to yeast cells rather loosely, and the bound HM-1 molecules can be removed from the cells by centrifugation. Almost the same results were obtained with aculeacin A (Fig. 5B). However, a slightly different feature was observed with papulacandin B (Fig. 5C) which perhaps indicates a stronger binding to the cells, as removal of the compound from the bound cells was difficult by centrifugation alone in a YPD medium.

Morphological Changes in HM-1-Treated Cells—Morphological changes in *S. cerevisiae* cells were investigated with a phase-contrast light microscope after incubating the cells with HM-1. When HM-1-treated cells were stained with methylene blue, many cells showed dye-stained

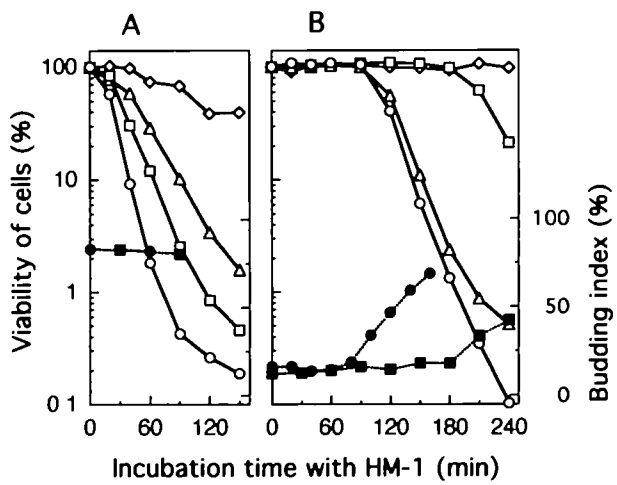

Fig. 2. **Conditions that affect HM-1 killer activity and yeast budding.** Killer activity and yeast budding were monitored as described in "MATERIALS AND METHODS." A: *S. cerevisiae* cells in the logarithmic growth phase were incubated with HM-1 at various temperatures as described in "MATERIALS AND METHODS." Viability of cells: △, 37°C; ○, 30°C; □, 20°C; ◇, 0°C. Budding index was determined for the cells cultured in the same medium in the absence of HM-1: ●, 30°C; ■, 20°C. B: *S. cerevisiae* cells in the resting state were incubated as in A. Symbols designating the incubation temperature are the same as in A.

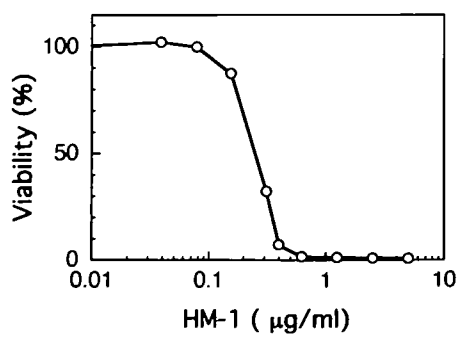

Fig. 3. **Viability of *S. cerevisiae* in the YPD medium containing HM-1.** *S. cerevisiae* cells (4×10^6 cells/ml) were cultured with various concentrations of HM-1 in YPD medium at 30°C with shaking at 175 rpm for 14 h. The viability of the cells was assessed after culturing by measuring the absorbance at 600 nm.

material not only inside the cell, but also apparently released or discharged from the cell (Fig. 6). Cells showing such discharge amounted to 50-60% of the total cells counted under a microscope. For a closer look at this peculiar event on the surface of HM-1-treated cells, we performed a scanning electron microscopic analysis (Fig. 7, A-D). As shown by phase-contrast microscopy in Fig. 6, the discharging region was confined to the budding area, especially on the top of the buds. We surveyed more than 100 specimens that contained damaged cells, and no other area showed discharges. These results showed that the budding site, especially the growing end, seems to be the area destroyed by HM-1, although it is not clear whether the HM-1 acts on this region directly or indirectly. In one of the cells in Fig. 7 (Panel C), scars marking a site of previous budding can be seen. However, such a historic site of budding was no longer a site of damage.

Effect of Osmotic Pressure and Salt—The electron microscopic pictures prompted us to examine the effect of osmotic pressure on the cells incubated with HM-1. Yeast cells were incubated in an isotonic medium containing 0.8 M sorbitol, and were compared with cells incubated under the standard conditions in a hypotonic YPD medium (Fig. 8). By adding sorbitol, the number of viable cells was increased by about 5-fold, when compared after 60 min incubation with cells cultured under the standard conditions (*control* in Fig. 8). These results indicated that the

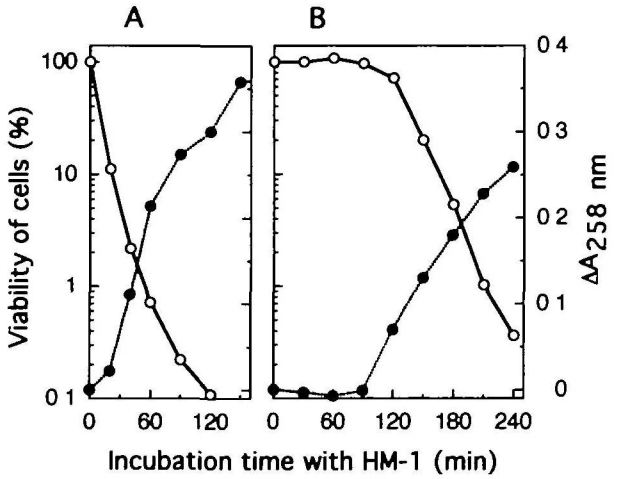

Fig. 4 **Leakage of cellular components into the medium and the viability of the cells.** Measurement of the ultraviolet light-absorbing materials and the number of viable cells were described in "MATERIALS AND METHODS." A· *S. cerevisiae* cells in the logarithmic growth phase were incubated with HM-1 ○, viability of cells; ●, increased UV_{258nm} absorbance in the medium. B *S cerevisiae* cells in the resting state were incubated as in A. Symbols designating the viability of cells and the increased UV_{258nm} absorbance are the same as in A.

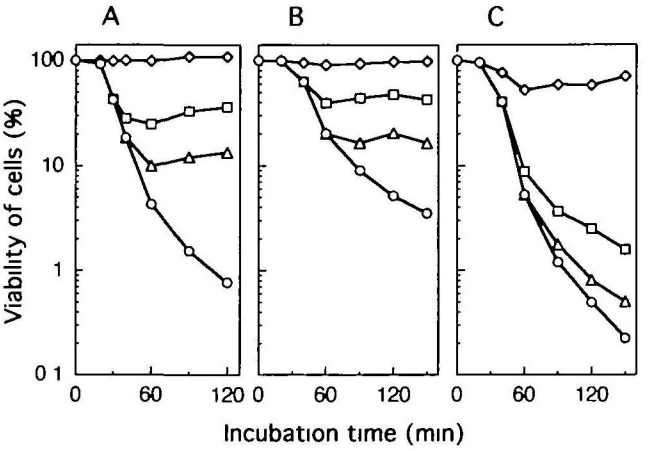

Fig. 5. **Effect of washing on the cytocidal activity of HM-1, aculeacin A, and papulacandin B.** Killer activity was monitored as described in "MATERIALS AND METHODS." *S. cerevisiae* cells in a rapidly growing state were incubated with HM-1 (4 μg/ml), aculeacin A (24 μg/ml), or papulacandin B (20 μg/ml) at 37°C. At the time of washing, a portion of the cells was withdrawn and centrifuged at 4,000 rpm for 5 min at 25°C The supernatant was removed and the precipitate was suspended with the same volume of YPD medium. This washing was repeated once, then the viability of the suspended cells was monitored by the standard liquid culture method. A: Effect on HM-1. ○, control; ◇, washed at 0 min; □, washed at 30 min; △, washed at 40 min B Effect on aculeacin A ○, control; ◇, washed at 20 min; □, washed at 40 min; △, washed at 60 min C: Effect on papulacandin B. ○, control; ◇, washed at 20 min; □, washed at 40 min, △, washed at 60 min.

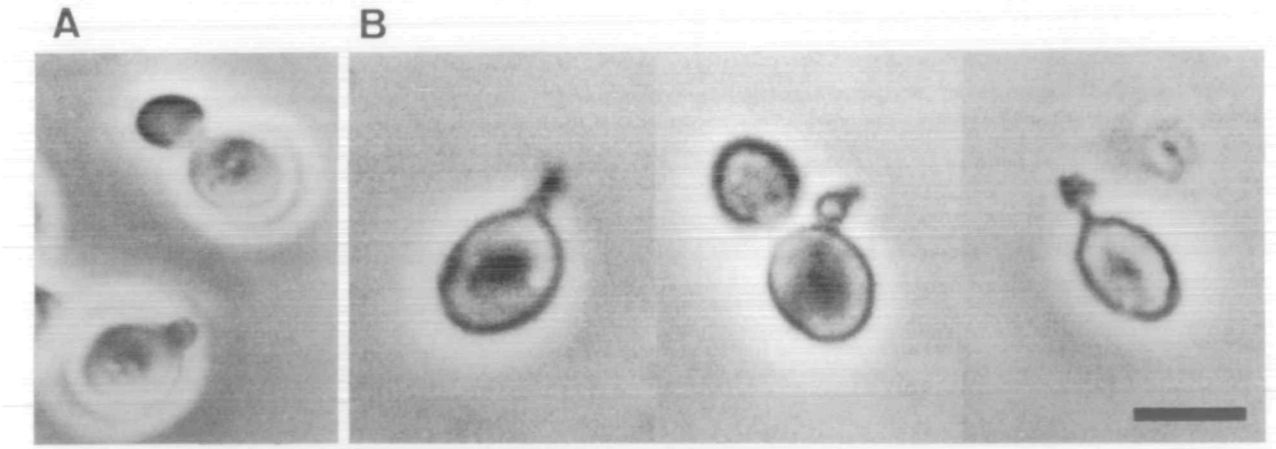

Fig. 6. **Phase-contrast microscopy of the HM-1-treated *S. cerevisiae* cells.** Sample preparation was described in "MATERIALS AND METHODS." A, normal cells; B, HM-1 treated cells. The bar indicates a length of 5 μm

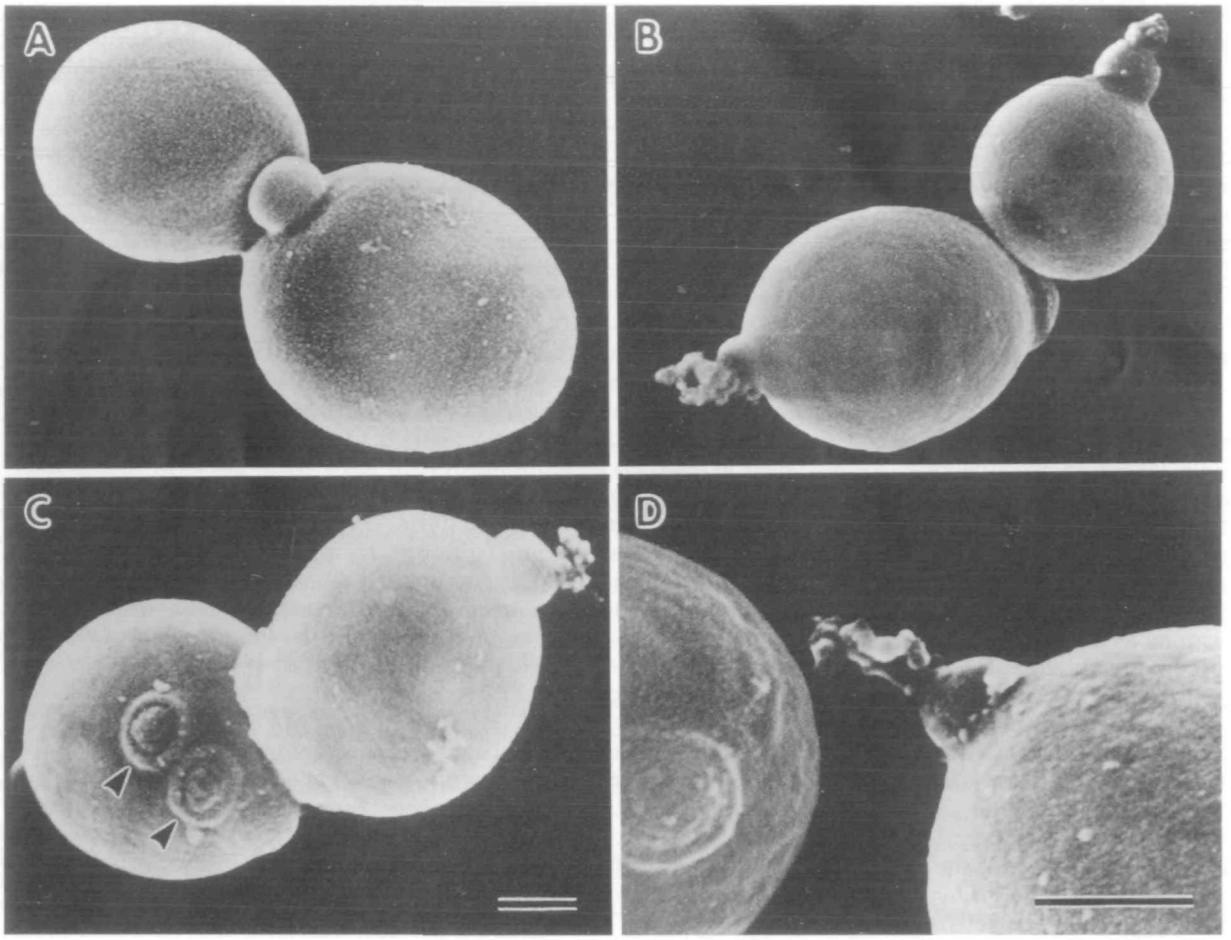

Fig. 7. **Scanning electron microscopy of *S. cerevisiae* cells.** Preparation of samples was described in "MATERIALS AND METHODS." A, normal cells, B, C, and D, HM-1 treated cells. A, B, and C are the same magnifications, and the bar indicates a length of 1 μm. The arrowhead shows the scars.

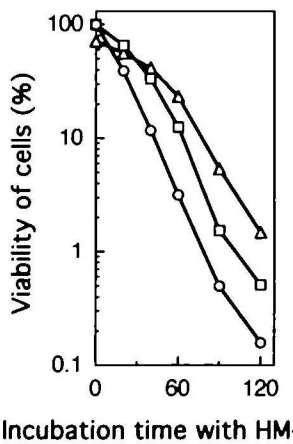

Fig. 8. **Effect of sorbitol and NaCl on HM-1 killer activity.** HM-1 killer activity was monitored by the standard liquid culture method as described in "MATERIALS AND METHODS." Sorbitol (0.8 M) and NaCl (0.15 M) were added to the incubation mixture as well as to the following culture medium. ○, control; □, plus sorbitol (to 0.8 M), △, plus NaCl (to 0.15 M).

HM-1-treated cells had probably burst out at the top of the buds, due to the osmotic pressure. We also tested sodium chloride as an osmotic stabilizer, and found that sodium chloride at 0.15 M (an isotonic condition for mammalian cells) reduced the cytocidal effect of HM-1, while the growth of yeast cells was down-regulated.

DISCUSSION

In this paper, we have described the mechanism underlying a peculiar cytocidal phenomenon caused by HM-1. HM-1 exerted a strong lethal effect on yeast A451 cells at a low concentration ($IC_{50} = 2.1 \times 10^{-8}$ M), an effect stronger than those of aculeacin A and papulacandin B, which were the most effective antifungal agents previously known (*14, 15*). The effect is cytocidal, and does not seem to retard the cell growth as judged from the results obtained with the plate assays shown in Fig. 1. The cytocidal effect of HM-1 was found to be cell cycle-dependent, or at least dependent on the proliferation of cells (Figs. 2 and 4). Cells in the resting state are apparently resistant to HM-1, and needed a lag time of about 90 min, corresponding to one cell cycle of replication, before becoming sensitive. These results indicated that some of the cell cycle stages may be impaired by HM-1, resulting in cell death. The direct cause of cell death appears to be pores that develop on the growing point of the bud, giving rise to a leak of cytosolic materials owing

(*32*) or the end-to-end interaction among tropomyosin molecules which would affect crossbridge attachment along the thin filament (*33*), no experimental evidence has been provided yet. The present results show that a positive feedback interaction between myosin crossbridge attachment to actin and Ca^{2+} binding to TN·C is markedly reduced upon substituting cardiac TN·C into fast skeletal myofibrils, and this may cause a decrease in the cooperativity of Ca^{2+}-regulation of contractile response.

MATERIALS AND METHODS

Substitution of Purified Cardiac TN·C into Fast Skeletal Myofibrils—Fast skeletal muscle myofibrils were prepared from back and leg muscles of male albino rabbits according to the modification by Harigaya *et al.* (*34*) of the method of Perry (*35*). The prepared myofibrils were suspended in 50% (v/v) glycerol, stored at −20°C for at least 2 weeks and used for the experiments. Cardiac TN·C was prepared from the left ventricles of porcine heart as described by Tsukui and Ebashi (*36*). Endogenous TN·C in fast skeletal myofibrils was extracted by *trans*-1,2-cyclohexanediamine-*N,N,N′,N′*-tetraacetic acid (CDTA) treatment and the CDTA-treated fast skeletal myofibrils were reconstituted with purified cardiac TN·C as described previously (*14, 27*). Briefly, TN·C was extracted three times by incubating myofibrils for 15 min at 25°C in a solution containing 40 mM Tris, 5 mM CDTA, 15 mM 2-mercaptoethanol, 200 μM phenylmethylsulfonyl fluoride, 1 μg/ml pepstatin A, and 0.6 mM NaN_3 (pH of the solution was around 8.4 and was not adjusted with either acid or base). The CDTA-treated myofibrils were reconstituted with TN·C by incubating them for 15 min under ice-cold conditions in a solution containing an excess amount of purified TN·C, followed by intensive washing out of unbound or nonspecifically bound TN·C by centrifugation and resuspension. Selective extraction of myosin from the CDTA-treated fast skeletal myofibrils and reconstitution with purified cardiac TN·C were carried out as described previously (*29*).

SDS-PAGE—SDS-PAGE was carried out at 12% polyacrylamide concentration according to the method of Laemmli (*37*). The gel was stained with Coomassie Brilliant Blue R-250 and scanned with a dual-wavelength scanning densitometer (Shimadzu CS-9000).

Measurements of Ca^{2+} Binding to TN·C in Myofibrils and Myofibrillar ATPase Activity—Ca^{2+} binding to TN·C in myofibrils was measured according to the procedure described previously (*27-30*). Briefly, the amount of Ca^{2+} bound to TN·C in myofibrils was determined by subtracting the amount of Ca^{2+} which was bound to TN·C-extracted (CDTA-treated) myofibrils from that bound to TN·C-reconstituted myofibrils. Since most of the TN·C molecules are specifically extracted in CDTA-treated myofibrils, this novel method allows us to determine the Ca^{2+} binding specific to TN·C even in the presence of large background Ca^{2+} binding to other myofibrillar proteins.

Ca^{2+}-binding measurements were carried out at 25°C in 5 ml of a solution containing either 1 mg/ml intact (myosin-unextracted) myofibrils in the presence and absence of ATP or 0.5 mg/ml myosin-extracted myofibrils in the absence of ATP. The free Mg^{2+} concentration and ionic strength were kept at 2.2 mM and 0.17 M, respectively. The solution also contained 20 mM 4-morpholinepropanesulfonic acid/NaOH (pH 7.0), 0.1 mg/ml creatine kinase, 10 mM creatine phosphate, 0.1 mM dithiothreitol, 10 mM glucose, 0.3 μCi/ml ^{45}Ca, 0.6 μCi/ml [^{3}H]glucose, 0.1 mM EGTA, varied amounts of $CaCl_2$ and either 100 mM KCl, 5 mM $MgCl_2$, 2 mM ATP in the presence of ATP or 161 mM KCl, 2.2 mM $MgCl_2$ in the absence of ATP. The myofibrillar ATPase activity was measured at 25°C in 2 ml of solution containing 1 mg/ml myofibrils, 20 mM 4-morpholinepropanesulfonic acid/NaOH (pH 7.0), 100 mM KCl, 5 mM $MgCl_2$, 2 mM ATP, 0.1 mg/ml creatine kinase, 10 mM creatine phosphate, 0.1 mM dithiothreitol, 10 mM glucose, 0.1 mM EGTA, and varied amounts of $CaCl_2$. The reaction was started by the addition of ATP and then stopped after 5 min of incubation by the addition of 2 ml of ice-cold 20% trichloroacetic acid containing 4% ascorbic acid. Liberated inorganic phosphate was measured by the method of Baginski *et al.* (*38*). The free Ca^{2+} concentration in the solution was calculated with the aid of a computer using the absolute binding constants for multiple ionic equilibria as described previously (*15*).

^{125}I-Labeling of Purified Cardiac TN·C—Purified porcine cardiac TN·C (0.5 mg) in 0.5 ml of 0.1 M potassium phosphate buffer (pH 8.5) was added to the Bolton and Hunter reagent in about 30 μl of benzene which had been evaporated in a microvial, agitated for 15 min on ice, and allowed to stand for 1 h on ice and overnight at 4°C. The ^{125}I-labeled TN·C (0.1 ml) was mixed with 2.5 ml of 8 mg/ml cold TN·C, extensively dialyzed against 1 mM $NaHCO_3$, and used to estimate the contents of TN·C in reconstituted myofibrils in the Ca^{2+} binding measurements.

Determination of the Protein Concentration—The protein concentrations of TN·C and myofibrils were determined by the Bio-Rad protein assay method and the biuret method, respectively. Calibration was done by amino acid analysis of these proteins.

RESULTS AND DISCUSSION

SDS-PAGE followed by gel scans showed that endogenous TN·C in fast skeletal myofibrils was fully displaced by a stoichiometric amount of cardiac TN·C and approximately 50% of the myosin light chain 2 was extracted following the CDTA treatment and the reconstitution with purified cardiac TN·C (Fig. 1A and Table I). Since it was confirmed in previous studies that the removal of approximately 50% of the myosin light chain 2 has no effect on the Ca^{2+}-regulation of the fast skeletal myofibrillar ATPase (*14, 39, 40*), all experiments reported here have been carried out with partially myosin light chain 2-extracted myofibrillar preparations.

Figure 2 shows the representative Ca^{2+} dependence of fast skeletal myofibrillar ATPase activity regulated by either fast skeletal or cardiac TN·C. In accordance with the previous studies (*13, 14*), cardiac TN·C gave a much less steep (*i.e.*, less cooperative) relationship between ATPase activation and free Ca^{2+} than fast skeletal TN·C; Hill coefficients (n_H) were 1.12 ± 0.07 (mean ± SE, $n=4$) and 2.05 ± 0.15 (mean ± SE, $n=3$) for cardiac and fast skeletal TN·C, respectively. Further, cardiac TN·C could activate the ATPase only partially compared to fast skeletal TN·C, in agreement with the previous studies on myofibrillar ATPase activity (*14, 41, 42*) or tension development of

skinned muscle fibers (*43*); the maximum ATPase activity with cardiac TN·C [0.419±0.017 μmol P_i/min/mg (mean±SE, $n=4$)] was about half of that with fast skeletal TN·C [0.801±0.044 μmol/min/mg (mean±SE, $n=3$)].

Figure 3 shows the Ca^{2+} binding to cardiac TN·C inserted into fast skeletal myofibrils under various conditions. Ca^{2+} binding was measured to TN·C in intact (myosin-unextracted) myofibrils in the presence and absence of ATP, and also to TN·C in myosin-extracted myofibrils in order to assess the effects of actin-myosin interactions; SDS-PAGE followed by gel scans showed that more than 90% of the myosin was extracted as estimated from the myosin light-chains contents, and that nearly stoichiometric amounts of cardiac TN·C were substituted into the myosin-extracted fast skeletal myofibrils (Fig. 1B and Table II). Ca^{2+} binding to TN·C in intact myofibrils in the presence of ATP and to TN·C in myosin-extracted myofibrils showed clear inflection points at about the 70% saturation level, which indicated that two classes of Ca^{2+}-binding sites with different affinity exist. Thus, the following equation was fitted to the Ca^{2+}-binding data by means of a non-linear least-squares method, assuming that there are two classes of binding sites with cooperativity:

$$B=\sum_{i=1}^{2}\frac{Ni(Ki[Ca^{2+}])^{n_{Hi}}}{1+(Ki[Ca^{2+}])^{n_{Hi}}} \quad (1)$$

where B is the total amount of bound Ca^{2+} as a function of free Ca^{2+} concentration ($[Ca^{2+}]$), and Ni, Ki, and n_{Hi} are the Ca^{2+} binding capacity, the apparent binding constant (reciprocal of the free Ca^{2+} concentration required for half-maximal binding) and the Hill coefficient of each class of binding site, respectively. The solid curves in Fig. 3 represent the best fits and the obtained Ca^{2+}-binding

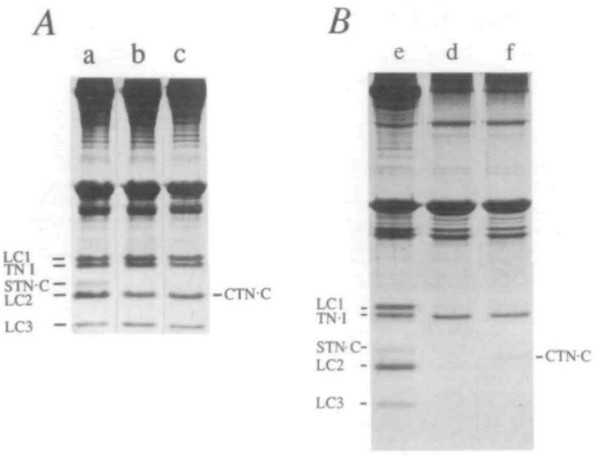

Fig 1. **Substitution of purified cardiac TN·C into (A) intact and (B) myosin-extracted fast skeletal myofibrils.** a and e, untreated control myofibrils, b, CDTA-treated myofibrils, c, CDTA-treated myofibrils reconstituted with purified cardiac TN·C; d, CDTA-treated and myosin-extracted myofibrils; f, CDTA-treated and myosin-extracted myofibrils reconstituted with purified cardiac TN·C Abbreviations: STN·C and CTN·C, fast skeletal and cardiac TN·C, respectively; TN·I, troponin I, LC1, LC2, and LC3, myosin light chains 1, 2, and 3, respectively.

TABLE I. **Relative contents of TN·C and LC2 in myofibrils before and after CDTA-treatment and after reconstitution with cardiac TN·C.** Densitometric scans were performed on the gel in Fig. 1A and the relative contents of TN·C and myosin light chain 2 (LC2) were obtained by normalizing the peak areas of TN·C and LC2 to the sum of peak areas of myosin light-chains 1 and 3.

Myofibrils	TN·C	LC2
Untreated	0 20	0.83
CDTA-treated	0 02	0 52
Reconstituted with cardiac TN·C	0.21[a]	(0 52)

[a]Cardiac TN·C comigrated with fast skeletal LC2 so that the relative content of cardiac TN·C was calculated assuming that the relative contents of LC2 in the CDTA-treated myofibrils before and after reconstitution with cardiac TN·C were the same.

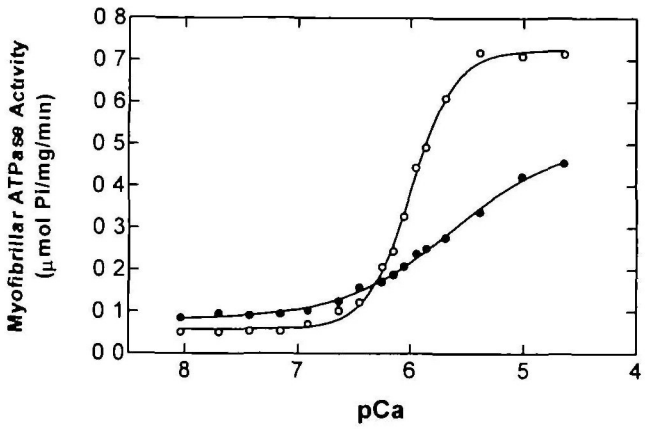

Fig. 2. **Ca^{2+} dependence of fast skeletal myofibrillar ATPase activity regulated by either fast skeletal or cardiac TN·C.** The CDTA-treated fast skeletal myofibrils were reconstituted with purified fast skeletal TN·C (○) or cardiac TN·C (●) and the myofibrillar ATPase activity was measured in the presence of varied amounts of Ca^{2+} as described in "MATERIALS AND METHODS."

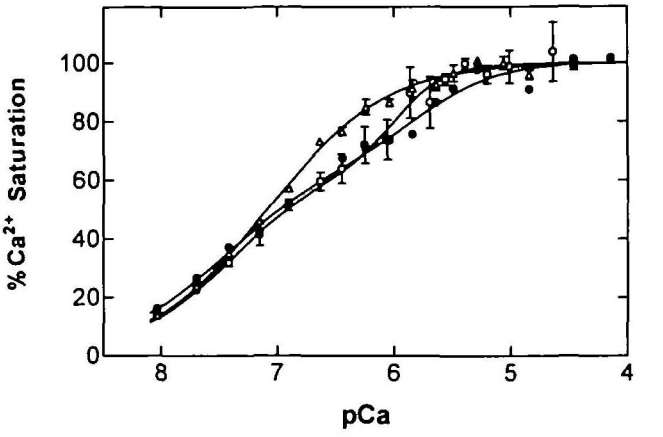

Fig. 3. **Ca^{2+} binding to cardiac TN·C inserted into fast skeletal myofibrils.** Ca^{2+} binding was measured to TN·C in intact (myosin-unextracted) myofibrils in the presence (○) and absence (△) of ATP and to TN·C in myosin-extracted myofibrils (●), with the double isotope technique using ^{45}Ca and [^{3}H]glucose as described in "MATERIALS AND METHODS," and normalized to the maximum amounts of bound Ca^{2+}. The error bars show the standard errors of the means for three determinations. Data for the myosin-extracted myofibrils are from one experiment. The solid curves were drawn using the average values listed in Table III which were obtained by fitting the individual Ca^{2+}-binding data to a model assuming cooperativity, as described by Eq. 1.

parameters are summarized in Table III.

In myosin-extracted myofibrils, the apparent Ca^{2+}-binding constant of the class-1 binding sites is about 40 times larger than that of the class-2 binding sites. In intact myofibrils, the affinity of class-2 binding sites is enhanced slightly in the presence of ATP and greatly in the absence of ATP, while class-1 binding sites show almost the same affinity as in myosin-extracted myofibrils. Although experimental errors are relatively large, the class-2 binding sites appear to show a positive cooperativity with a Hill coefficient of 2.1 only in the presence of ATP. The Ca^{2+}-binding capacities of classes 1 and 2 are in a ratio of close to 2:1 in all cases. TN·C content in the reconstituted myofibrils precipitated by centrifugation in the Ca^{2+}-binding measurements, which was estimated by using ^{125}I-labeled TN·C, was 0.58 ± 0.01 (mean$\pm$SE, $n=3$) μmol/g in intact myofibrils in the presence of ATP. Thus, the amounts of Ca^{2+} bound to classes 1 and 2 are almost equivalent to 2 and 1 mol Ca^{2+}/mol TN·C, respectively, suggesting that the classes 1 and 2 correspond to the high-affinity sites (sites III and IV) and the single low-affinity site (site II), respectively, of cardiac TN·C. The extra sum of squares principle F test (*44*) showed that the cooperative model described by Eq. 1 provides a statistically significantly better fit than a simpler model without assuming cooperativity, which is described by Eq. 1, setting $n_H i=1$ and $N_1/N_2=2$, at a level of significance of 0.5%. These results indicate that in the presence of ATP, Ca^{2+} binding to only the single low-affinity site of cardiac TN·C is enhanced by the feedback from myosin crossbridge interactions with actin in fast skeletal myofibrils, in accordance with the idea originally proposed by Bremel and Weber for the cooperative Ca^{2+}-activation of fast skeletal muscle (*32*).

Ca^{2+}-activation of ATPase of fast skeletal myofibrils regulated by cardiac TN·C and Ca^{2+} binding to class-2 sites in the presence of ATP were found to occur in roughly the same free Ca^{2+} concentration range, while Ca^{2+} binding to class-1 sites almost reached a plateau before the activation of ATPase (Fig. 4). This suggests that the site II of cardiac TN·C is responsible for the Ca^{2+}-regulation of ATPase activity in fast skeletal myofibrils as well as in cardiac myofibrils (*30*). The Ca^{2+}-activation of myofibrillar ATPase, however, occurred at slightly higher Ca^{2+} concentrations with less cooperativity ($K=4.4\pm1.9\times10^5$ M^{-1}, $n_H=1.12\pm0.07$; mean$\pm$SE, $n=4$), as compared to the Ca^{2+} binding to class-2 sites. It has been suggested that the activation of ATPase of fast skeletal myofibrils regulated with fast skeletal TN·C could be nearly proportional to the Ca^{2+} binding to site II of TN·C (*29*). This might suggest that, due to a lower degree of coupling between Ca^{2+} binding to TN·C and activation of ATPase, more cardiac TN·C molecules compared to fast skeletal TN·C have to be saturated by Ca^{2+} to turn on the thin filaments in fast skeletal myofibrils to a given degree, although more detailed analysis should be done using theoretical models based on the nearest-neighbor protein-protein interactions in the thin filaments (*45-47*). Cooperative Ca^{2+} binding to a single low-affinity class-2 site ($n_H=2$) suggests that some cooperative interactions are present along the thin filaments.

Ca^{2+} binding to the low-affinity site(s) of TN·C is generally thought to be responsible for the Ca^{2+} regulation of contraction in cardiac and skeletal muscles. Several investigators have shown that cycling and rigor myosin

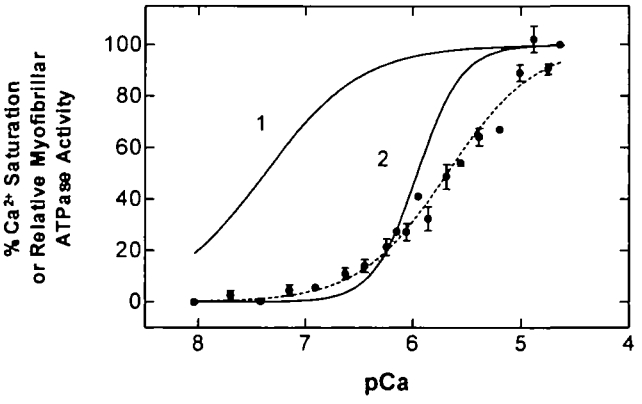

Fig. 4. **A comparison of Ca^{2+}-activated fast skeletal myofibrillar ATPase regulated by cardiac TN·C with Ca^{2+} binding in the presence of ATP to class 1 and 2 sites of cardiac TN·C in myofibrils.** The ATPase activity of the CDTA-treated fast skeletal myofibrils reconstituted with purified cardiac TN·C (●) was measured under the same conditions as those used for the Ca^{2+}-binding measurements in the presence of ATP. The data points represent the mean$\pm$SE for four determinations. The Ca^{2+}-binding curves of the class-1 sites (curve 1) and class-2 sites (curve 2) of TN·C in myofibrils were computed using the average values of the Ca^{2+}-binding parameters listed in Table III.

TABLE II. **Relative contents of myosin light-chains and TN·C in myosin-extracted fast skeletal myofibrils.** Densitometric scans were performed on the gel in Fig. 1B and the relative contents of myosin light chains and TN·C were obtained by normalizing the peak areas of myosin light chains and TN·C to the peak area of troponin I. Abbreviations: LC1, LC2, and LC3, myosin light chains 1, 2, and 3, respectively.

Myofibrils	LC1	LC2	LC3	TN·C
Untreated	1.11	1.27	0.35	0.20
CDTA-treated and myosin-extracted	0.10	0.08	0.03	0.02
Reconstituted with cardiac TN·C	0.08	0.06	0.00	0.23

TABLE III. **Ca^{2+}-binding parameters of cardiac TN·C in fast skeletal myofibrils.** Ca^{2+}-binding capacity (N), apparent Ca^{2+}-binding constant (K) and Hill coefficient (n_H) are presented as mean$\pm$SE of the values obtained by fitting the data shown in Fig. 3 to the Eq. 1.

Conditions	Class 1			Class 2		
	N_1 (μmol/g myof. mol/mol TN·C)	K_1 ($\times10^7$ M^{-1})	n_{H1}	N_2 (μmol/g myof. mol/mol TN·C)	K_2 ($\times10^6$ M^{-1})	n_{H2}
−Myosin	1.44 (0.56[a])	2.85 (2.62[a])	0.87 (0.45[a])	0.67 (0.27[a])	0.59 (0.22[a])	1.29 (0.50[a])
+Myosin						
+ATP	1.08$\pm$0.04 (1.86$\pm$0.08)	2.40$\pm$0.14	0.96$\pm$0.03	0.52$\pm$0.02 (0.90$\pm$0.04)	0.96$\pm$0.39	2.12$\pm$0.38
−ATP	1.24$\pm$0.02	1.97$\pm$0.34	0.88$\pm$0.01	0.67$\pm$0.01	5.39$\pm$1.27	0.95$\pm$0.12

[a]Asymptotic standard errors of each parameter obtained by curve-fitting.

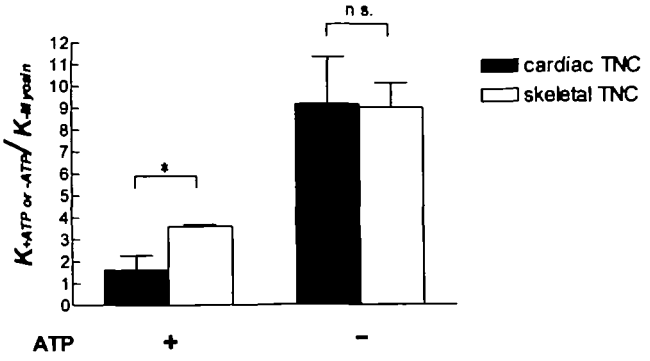

Fig. 5. **Effects of actin-myosin interactions in the presence and absence of ATP to enhance the Ca^{2+} affinities of site II of cardiac TN·C and the low-affinity sites of fast skeletal TN·C in fast skeletal myofibrils.** $K_{+ATP\ or\ -ATP}$ and $K_{-Myosin}$ are the apparent Ca^{2+}-binding constants of site II of cardiac TN·C or low-affinity sites of fast skeletal TN·C, in intact myofibrils in the presence or absence of ATP and in myosin-extracted myofibrils, respectively. Each column represents the mean with SE of three determinations. $^*p < 0.05$, by unpaired (or Welch's) t test.

crossbridges induce a conformational change or an increase in the Ca^{2+}-binding affinity of the low-affinity site(s) of cardiac and fast skeletal muscle TN·C in myofibrils and muscle fibers (*22, 24, 25, 32, 48-50*). Fuchs and Wang (*26*), however, observed no statistically significant effect of cycling crossbridges on the Ca^{2+} binding to fast skeletal TN·C in skinned fast skeletal muscle fibers. In contrast, we have previously shown that the Ca^{2+} binding to the low-affinity sites of fast skeletal TN·C in fast skeletal myofibrils is definitely enhanced by myosin crossbridge interaction with actin both in the presence and absence of ATP (*29*). This discrepancy is probably due to the differences in methods or preparations. While we evaluated the Ca^{2+} binding to TN·C by measuring the amounts of Ca^{2+} bound to the TN·C-extracted (CDTA-treated) myofibrils in order to subtract the large background activity of myofibrillar Ca^{2+} binding from total bound Ca^{2+}, Fuchs and Wang only measured the total bound Ca^{2+} in skinned muscle fibers under conditions in which Ca^{2+} binding to myosin, the major component of background myofibrillar Ca^{2+} binding, was expected to be small and negligible, but high- and low-affinity sites of TN·C could no longer be distinguished. Furthermore, they used skinned muscle fibers in which it seems more difficult to measure biochemically the direct Ca^{2+} binding to TN·C compared to the isolated myofibrils we used. Figure 5 compares the effects of myosin crossbridge attachment in fast skeletal myofibrils on the Ca^{2+} affinities of site II of cardiac TN·C and the low-affinity sites of fast skeletal TN·C. The Ca^{2+} affinities of site II of cardiac TN·C and the low-affinity sites of fast skeletal TN·C were greatly enhanced (by 8-9 times) in the absence of ATP and the difference between them was not statistically significant. Although the enhancement effects were quite small in the presence of ATP, the Ca^{2+} affinity of the low-affinity sites of fast skeletal TN·C was still enhanced by 3.6 times, while the Ca^{2+} affinity of site II of cardiac TN·C was enhanced by only 1.4 times. The difference in the effects of ATP on the Ca^{2+} affinities of fast skeletal TN·C and cardiac TN·C was statistically significant. These results indicate that the feedback mechanism between myosin crossbridge attachment and Ca^{2+} binding to TN·C in the presence of ATP does not fully function in the cardiac TN·C-substituted fast skeletal myofibrils, as compared with the fast skeletal TN·C-reconstituted fast skeletal myofibrils. This lower degree of coupling between myosin and cardiac TN·C as compared to myosin and fast skeletal TN·C could result in a lower overall myofibrillar ATPase activity and a lower cooperativity in Ca^{2+} regulation of myofibrillar ATPase (Fig. 2) as well as a smaller increase in Ca^{2+} affinity of the low-affinity sites of TN·C.

In conclusion, the present findings provide strong evidence that a reduction in the positive feedback interactions between myosin crossbridge attachment to actin and Ca^{2+} binding to the regulatory site of TN·C is involved in the previously found phenomenon that the insertion of cardiac TN·C into fast skeletal muscle causes marked reduction in cooperativity of Ca^{2+} regulation and overall ATPase activity or tension development in myofibrils (*14, 41, 42*) and skinned muscle fibers (*13, 43*). It has been shown that restoration of Ca^{2+}-binding ability of inactive site I in cardiac TN·C by site-directed mutagenesis imparts fast skeletal TN·C-like properties in terms of cooperativity, *i.e.*, a marked increase in cooperativity of Ca^{2+}-regulation, in slow skeletal (*31*) and cardiac (*51*) muscles, but cannot fully activate fast skeletal muscle myofibrils (*43*). Thus, the lower degree of coupling between myosin and cardiac TN·C is not due to the deficient Ca^{2+} coordination in site I of cardiac TN·C but may be due to some other structural difference between cardiac and fast skeletal TN·Cs. Further studies with protein-engineering techniques directed toward clarifying the structural difference between cardiac and fast skeletal TN·Cs which is involved in the different degree of coupling between myosin and TN·C will contribute to a clearer understanding of the regulatory mechanism of contraction in both skeletal and cardiac muscles.

REFERENCES

1. Ebashi, S., Kodama, A., and Ebashi, F. (1968) Troponin. I. Preparation and physiological function. *J. Biochem.* **64**, 465-477
2. Ebashi, S., Endo, M., and Ohtsuki, I. (1969) Control of muscle contraction. *Q. Rev. Biophys.* **2**, 351-384
3. Ebashi, S., Ohtsuki, I., and Mihashi, K. (1972) Regulatory proteins of muscle with special reference to troponin. *Cold Spring Harbor Symp. Quant. Biol.* **37**, 215-223
4. Ohtsuki, I., Maruyama, K., and Ebashi, S. (1986) Regulatory and cytoskeletal proteins of vertebrate skeletal muscle. *Adv. Protein Chem.* **38**, 1-67
5. Collins, J.H., Greaser, M.L., Potter, J.D., and Horn, M.J. (1977) Determination of the amino acid sequence of troponin C from rabbit skeletal muscle. *J. Biol. Chem.* **252**, 6356-6362
6. Potter, J.D. and Gergely, J. (1975) The calcium and magnesium binding sites on troponin and their role in the regulation of myofibrillar adenosine triphosphatase. *J. Biol. Chem.* **250**, 4628-4633
7. Leavis, P.C., Rosenfeld, S.S., Gergely, J., Grabarek, Z., and Drabikowski, W. (1978) Proteolytic fragments of troponin C. Localization of high and low affinity Ca^{2+} binding sites and interactions with troponin I and troponin T. *J. Biol. Chem.* **253**, 5452-5459
8. Sin, I.L., Fernandes, R., and Mercola, D. (1978) Direct identification of the high and low affinity calcium binding sites of troponin-C. *Biochem. Biophys. Res. Commun.* **82**, 1132-1139
9. Potter, J.D., Seidel, J.C., Leavis, P., Lehrer, S.S., and Gergely, J. (1976) Effect of Ca^{2+} binding on troponin C. Changes in spin label mobility, extrinsic fluorescence, and sulfhydryl reactivity.

J. Biol. Chem. **251**, 7551-7556
10. Holroyde, M.J., Robertson, S.P., Johnson, J.D., Solaro, R.J., and Potter, J.D. (1980) The calcium and magnesium binding sites on cardiac troponin and their role in the regulation of myofibrillar adenosine triphosphatase. *J. Biol. Chem.* **255**, 11688-11693
11. van Eerd, J.-P. and Takahashi, K. (1976) Determination of the complete amino acid sequence of bovine cardiac troponin C. *Biochemistry* **15**, 1171-1180
12. Kobayashi, T., Takagi, K., Konishi, S., Morimoto, S., and Ohtsuki, I. (1989) Amino acid sequence of porcine cardiac muscle troponin C. *J. Biochem.* **106**, 55-59
13. Moss, R.L., Lauer, M.R., Giulian, G.G., and Greaser, M.L. (1986) Altered Ca^{2+} dependence of tension development in skinned skeletal muscle fibers following modification of troponin by partial substitution with cardiac troponin C. *J. Biol. Chem.* **261**, 6096-6099
14. Morimoto, S. and Ohtsuki, I. (1987) Ca^{2+}- and Sr^{2+}-sensitivity of the ATPase activity of rabbit skeletal myofibrils: Effect of the complete substitution of troponin C with cardiac troponin C, calmodulin, and parvalbumins. *J. Biochem.* **101**, 291-301
15. Morimoto, S. and Ohtsuki, I. (1988) Effect of substitution of troponin C in cardiac myofibrils with skeletal troponin C or calmodulin on the Ca^{2+}- and Sr^{2+}-sensitive ATPase activity. *J. Biochem.* **104**, 149-154
16. Gulati, J., Scordilis, S., and Babu, Á. (1988) Effect of troponin C on the cooperativity in Ca^{2+} activation of cardiac muscle. *FEBS Lett.* **236**, 441-444
17. Kambara, M. (1994) Ca^{2+}- and Sr^{2+}-sensitive ATPase activity of slow skeletal myofibrils in comparison with fast skeletal and cardiac myofibrils. *Fukuoka Acta Med.* **85**, 5-14
18. Morimoto, S. and Ohtsuki, I. (1994) Role of troponin C in determining the Ca^{2+}-sensitivity and cooperativity of the tension development in rabbit skeletal and cardiac muscles. *J. Biochem.* **115**, 144-146
19. Holroyde, M.J., Howe, E., and Solaro, R.J. (1979) Modification of calcium requirements for activation of cardiac myofibrillar ATPase by cyclic AMP dependent phosphorylation. *Biochim. Biophys. Acta* **586**, 63-69
20. Solaro, R.J. and Rüegg, J.C. (1982) Stimulation of Ca^{2+} binding and ATPase activity of dog cardiac myofibrils by AR-L 115BS, a novel cardiotonic agent. *Circ. Res.* **51**, 290-294
21. Blanchard, E.M., Pan, B.-S, and Solaro, R.J. (1984) The effect of acidic pH on the ATPase activity and troponin Ca^{2+} binding of rabbit skeletal myofilaments. *J. Biol. Chem.* **259**, 3181-3186
22. Pan, B.-S. and Solaro, R.J. (1987) Calcium-binding properties of troponin C in detergent-skinned heart muscle fibers. *J. Biol. Chem.* **261**, 15883-15890
23. Fuchs, F. and Fox, C. (1982) Parallel measurements of bound calcium and force in glycerinated rabbit psoas muscle fibers. *Biochim. Biophys. Acta* **679**, 110-115
24. Hofmann, P.A. and Fuchs, F. (1987) Effect of length and cross-bridge attachment on Ca^{2+} binding to cardiac troponin C. *Am. J. Physiol.* **253**, C90-C96
25. Hofmann, P.A. and Fuchs, F. (1987) Evidence for a force-dependent component of calcium binding to cardiac troponin C. *Am. J. Physiol.* **253**, C541-546
26. Fuchs, F. and Wang, Y.-P. (1991) Force, length, and Ca^{2+}-troponin C affinity in skeletal muscle. *Am. J. Physiol.* **261**, C541-546
27. Morimoto, S. and Ohtsuki, I. (1989) Ca^{2+} binding to skeletal muscle troponin C in skeletal and cardiac myofibrils. *J. Biochem.* **105**, 435-439
28. Morimoto, S. (1991) The effect of Mg^{2+} on the Ca^{2+} binding to troponin C in rabbit fast skeletal myofibrils. *Biochim. Biophys. Acta* **1073**, 336-340
29. Morimoto, S. (1991) Effect of myosin cross-bridge interaction with actin on the Ca^{2+}-binding properties of troponin C in fast skeletal myofibrils. *J. Biochem.* **109**, 120-126
30. Morimoto, S. and Ohtsuki, I. (1994) Ca^{2+} binding to cardiac troponin C in the myofilament lattice and its relation to the myofibrillar ATPase activity. *Eur. J. Biochem.* **226**, 597-602
31. Putkey, J.A., Sweeney, H.L., and Campbell, S.T. (1989) Site-directed mutation of the trigger calcium-binding sites in cardiac troponin C. *J. Biol. Chem.* **264**, 12370-12378
32. Bremel, R.D. and Weber, A. (1972) Cooperation within actin filament in vertebrate skeletal muscle. *Nature New Biol.* **238**, 97-101
33. Walsh, T.P., Trueblood, C.E., Evans, R., and Weber, A. (1984) Removal of tropomyosin overlap and the co-operative response to increasing calcium concentrations of the acto-subfragment-1 ATPase. *J. Mol. Biol.* **182**, 265-269
34. Harigaya, S., Ogawa, Y., and Sugita, H. (1968) Calcium binding activity of microsomal fraction of rabbit red muscle. *J. Biochem.* **63**, 324-331
35. Perry, S.V. (1952) The bound nucleotide of the isolated myofibril. *Biochem. J.* **51**, 495-499
36. Tsukui, R. and Ebashi, S. (1973) Cardiac troponin. *J. Biochem.* **73**, 1119-1121
37. Laemmli, U.K. (1970) Cleavage of structural proteins during the assembly of the head of bacteriophage T4. *Nature* **227**, 680-685
38. Baginski, E.S., Foa, P.P., and Zak, B. (1967) Determination of phosphate: Study of labile organic phosphate interference. *Clin. Chim. Acta* **15**, 155-158
39. Morimoto, S., Fujiwara, T., and Ohtsuki, I. (1988) Restoration of Ca^{2+}-activated tension of CDTA-treated single skeletal muscle fibers by troponin C. *J. Biochem.* **104**, 873-874
40. Nakamura, Y., Shiraishi, F., and Ohtsuki, I. (1994) The effect of troponin C substitution on the Ca^{2+}-sensitive ATPase activity of vertebrate and invertebrate myofibrils by troponin Cs with various numbers of Ca^{2+}-binding sites. *Comp. Biochem. Physiol.* **108B**, 121-133
41. Kambara, M., Shiraishi, F., and Ohtsuki, I. (1990) Replacement of troponin C in fast skeletal myofibrils by troponin C from various muscles. *Biomed. Res.* **11**, 291-297
42. Shiraishi, F. and Tanokura, M. (1993) Effect of substitution of troponin C on the ATPase of bullfrog skeletal myofibrils with troponin C from various muscles. *Fukuoka Acta Med.* **84**, 345-348
43. Gulati, J., Babu, Á., and Putkey, J.A. (1989) Down-regulation of fast-twitch skeletal muscle fiber with cardiac troponin-C and recombinant mutants. Structure/function studies with site-directed mutagenesis. *FEBS Lett.* **248**, 5-8
44. Quast, U. and Horst, M. (1982) Interaction of [^{3}H]flunitrazepam with the benzodiazepine receptor: Evidence for a ligand-induced conformation change. *Biochem. Pharmacol.* **31**, 2761-2768
45. Tawada, Y. and Tawada, K. (1975) Co-operative regulation mechanism of muscle contraction: Inter-tropomyosin co-operation model. *J. Theor. Biol.* **50**, 269-283
46. Hill, T.L. (1983) Two elementary models for the regulation of skeletal muscle contraction by calcium. *Biophys. J.* **44**, 383-396
47. Shiner, J.S. (1986) A theoretical analysis of binding to the Ca^{2+}-specific sites on troponin incorporated into thin filaments. *Biophys. J.* **50**, 601-611
48. Güth, K. and Potter, J.D. (1987) Effect of rigor and cycling cross-bridges on the structure of troponin C and on the Ca^{2+} affinity of the Ca^{2+}-specific regulatory sites in skinned rabbit psoas fibers. *J. Biol. Chem.* **262**, 13627-13635
49. Allen, T.S., Yates, L.D., and Gordon, A.M. (1992) Ca^{2+}-dependence of structural changes in troponin-C in demembranated fibers of rabbit psoas muscle. *Biophys. J.* **61**, 399-409
50. Hannon, J.D., Martyn, D.A., and Gordon, A.M. (1992) Effects of cycling and rigor crossbridges on the conformation of cardiac troponin C. *Circ. Res.* **71**, 984-991
51. Gulati, J., Sonnenblick, E., and Babu, Á. (1990) The role of troponin C in the length dependence of Ca^{2+}-sensitive force of mammalian skeletal and cardiac muscles. *J. Physiol.* **441**, 305-324